Atmospheric Environment 206 (2019) 144–155

Contents lists available at ScienceDirect

Atmospheric Environment

journal homepage: www.elsevier.com/locate/atmosenv

Source attribution of black carbon affecting regional air quality, premature mortality and glacial deposition in 2000

Yue Qin[a], Yuanyuan Fang[b], Xiaoyuan Li[c], Vaishali Naik[d], Larry W. Horowitz[d], Junfeng Liu[e], Noah Scovronick[a], Denise L. Mauzerall[a,c,*]

[a] Woodrow Wilson School of Public Policy and International Affairs, Princeton University, Princeton, NJ, 08544, USA
[b] Bay Area Air Quality Management District, 375 Beale Street, San Francisco, CA 94105, USA
[c] Department of Civil and Environmental Engineering, Princeton University, Princeton, NJ, 08544, USA
[d] UCAR/NOAA Geophysical Fluid Dynamics Laboratory, Princeton, Princeton, NJ, 08540, USA
[e] College of Urban and Environmental Sciences, Peking University, Beijing, 100080, China

ARTICLE INFO

Keywords:
BC
Tagging method
Source-receptor matrix
Attribution efficiency
Human health

ABSTRACT

Black carbon (BC) mitigation can reduce adverse environmental impacts on climate, air quality, human health, and water resource availability. To facilitate the identification of mitigation priorities, we use a state-of-the-science global chemistry-climate coupled model (AM3), with additional tagged BC tracers representing regional (East Asia, South Asia, Europe and North America) and sectoral (land transport, residential, industry) anthropogenic BC emissions to identify sources with the largest impacts on air quality, human health and glacial deposition. We find that within each tagged region, domestic emissions dominate BC surface concentrations and associated premature mortality (generally over 90%), as well as BC deposition on glaciers (~40–95% across glaciers). BC emissions occurring within each tagged source region contribute roughly 1–2 orders of magnitude more to their domestic BC concentrations, premature mortality, and BC deposition on regional glaciers than that caused by the same quantity of BC emitted from foreign regions. At the sectoral level, the South Asian residential sector contributes ~60% of BC associated premature mortality in South Asia and ~40–60% of total BC deposited on southern Tibetan glaciers. Our findings imply that BC mitigation within a source region, particularly from East and South Asian residential sectors, will bring the largest reductions in BC associated air pollution, premature mortality, and glacial deposition.

1. Introduction

Climate change is a complex, long-term, and large-scale issue which is challenging to address in the short term due in part to the high political and economic costs of CO_2 mitigation (Keohane and Victor, 2016). However, mitigating black carbon (BC), which has a lifetime of only several days in the atmosphere and a strong positive direct regional radiative forcing, is recognized as an effective strategy to address near-term global warming by both the scientific and diplomatic communities (CCAC, 2012; EPA, 2012; Jacobson, 2002; Kopp and Mauzerall, 2010; Ramanathan and Carmichael, 2008; Huang et al., 2015). Additionally, BC mitigation has immediate benefits for air quality, human health and water resources (via impacts on glaciers), providing strong motivation for its near-term mitigation (Bond et al., 2013; Hansen and Nazarenko, 2004; Peng et al., 2016; Shindell et al., 2012; UNEP/WMO, 2011; Ding et al., 2016; Wang et al., 2018; Zhang et al., 2016; Huang et al., 2018). To help prioritize BC mitigation strategies, we quantify the regional and sectoral contributions of BC emissions on air quality, premature mortality and glacial deposition.

Epidemiological studies have linked long-term exposure to fine particulate matter in ambient air, of which BC is a key component, with an elevated risk of premature mortality (Hoek et al., 2013; Janssen et al., 2012; REVIHAAP, 2013). UNEP/WMO (2011)) and Shindell et al. (2012) identified potential BC mitigation measures and estimated that by 2030 a full global implementation of these measures could avoid 2.3 million premature deaths annually due to reduced outdoor air pollution. Both studies quantified the health benefits of BC abatement under future scenarios using $PM_{2.5}$ concentration-response functions from the American Cancer Society (ACS) cohort studies (Krewski et al., 2009). However, the relative risk of $PM_{2.5}$ exposure found in the ACS study, which is based on ambient concentrations typical of the U.S., does not accurately represent the risk associated with high levels of $PM_{2.5}$

* Corresponding author. Woodrow Wilson School of Public Policy and International Affairs, Princeton University, Princeton, NJ, 08544, USA.
E-mail address: mauzeral@princeton.edu (D.L. Mauzerall).

https://doi.org/10.1016/j.atmosenv.2019.02.048
Received 21 September 2018; Received in revised form 8 January 2019; Accepted 24 February 2019
Available online 09 March 2019
1352-2310/

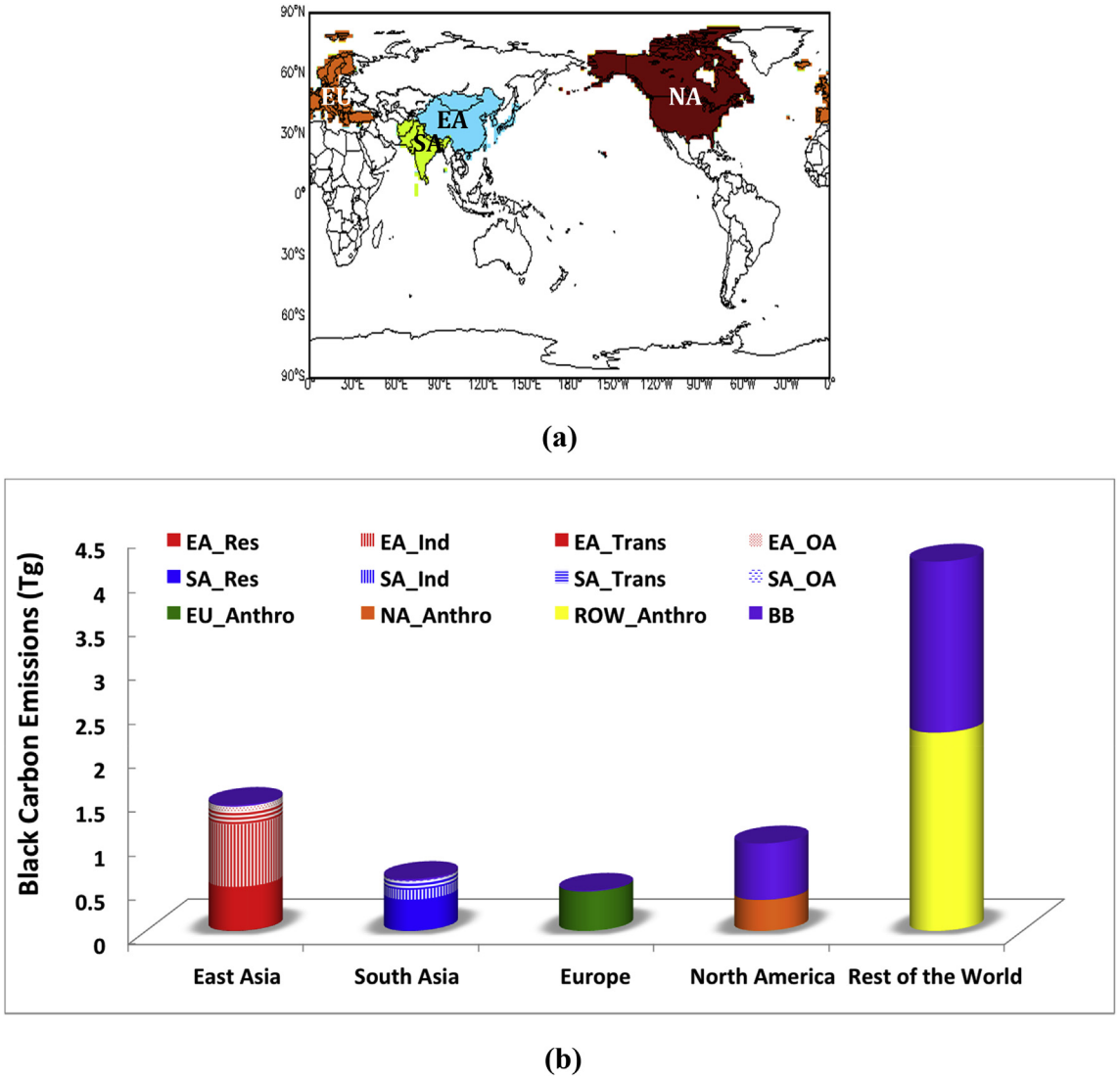

Fig. 1. (a) Location of the four-tagged regions: East Asia (EA), South Asia (SA), Europe (EU), and North America (NA). (b) Global annual mean land anthropogenic and biomass burning black carbon (BC) emissions (Tg) from our tagged regions and different sectors. Land anthropogenic (Anthro) sources include fossil fuel and biofuel from the residential (Res), industry (Ind), land transportation (Trans), and other (agricultural waste burning and waste management) (OA) sectors. BB (Biomass burning) emissions include forest and grassland fires. BB emissions are not tagged but are included in total BC emissions.

exposure in Asia, which is better represented in the Global Burden of Disease (GBD) analysis (Burnett et al., 2014). Here we conduct additional analyses of source attribution of regional and sectoral BC emissions to BC associated health effects, based on relative risks at both high and low levels of $PM_{2.5}$ exposures, in order to prioritize mitigation efforts.

In addition to air quality and health considerations, BC deposition on glaciers is also of immediate concern because of its effects on snow albedo, atmospheric radiative forcing, and the melting rates of snow and ice that may modify the seasonality and trends of melt-water supply (Kopacz et al., 2011; Ramanathan et al., 2005). Using the GEOS-Chem adjoint model, Kopacz et al. (2011) identified India and China as the primary emission sources of BC deposited on five glaciers in the Himalayas and Tibetan Plateau (HTP). Here we further characterize the regional and sectoral anthropogenic sources depositing BC on glaciers to prioritize BC mitigation.

This study goes beyond previous work and conducts an integrated assessment of the source attribution of regional and sectoral present-day (2000) BC emissions on air quality, premature mortality and deposition of BC on northern hemisphere glaciers. We apply a source-tagging approach within a fully coupled global 3-D chemistry-climate atmospheric model, Atmospheric Model version 3 (AM3) (Donner et al., 2011). This model allows us to evaluate inter-regional and inter-continental transport of BC from specific sources and regions and analyze their impacts during average conditions of climate and air quality around the year 2000 on air quality, health and glacial deposition. This, to our knowledge, is among the first trials, to conduct such an integrated assessment to evaluate the impact of BC globally.

The tagging technique has been applied in many literature (Brandt et al., 2012; Liu et al., 2005, 2009a; Wang et al., 2014) and the model (AM3/GFDL) we applied also has been applied in many recent atmospheric physics/chemistry, air quality and health studies (Fang et al., 2013; Lamarque et al., 2013a, 2013b; Lee et al., 2013; Naik et al., 2013; Parrish et al., 2014; Schnell et al., 2015; Shen et al., 2017; Shindell et al., 2013; Silva et al., 2013; Stevenson et al., 2013; Voulgarakis et al., 2013; Young et al., 2013). Using AM3, a climate-chemistry coupled model, we aim to reflect the average condition of climate and air quality around the year 2000. The simulation we conduct for this study is part of an extensive assessment of the impact of BC mitigation, not only on air quality, health and glacier deposition (as shown in this paper), but also on climate (Lamarque et al., 2013b; Lee et al., 2013). As a result, it uses a present-day (2000) emission inventory developed

for the Intergovernmental Panel on Climate Change Fifth Assessment Report (IPCC AR5) by Lamarque et al. (2010). The emission inventory used in our study is a standard one that the climate-chemistry community made and used in their work to simulate the 2000s climatology and chemistry (Fang et al., 2013; Lamarque et al., 2013a, 2013b; Lee et al., 2013; Naik et al., 2013; Parrish et al., 2014; Schnell et al., 2015; Shen et al., 2017; Shindell et al., 2013; Silva et al., 2013; Stevenson et al., 2013; Voulgarakis et al., 2013; Young et al., 2013). However, one thing to note is that this IPCC historical emission inventory, as reported by Lamarque et al. (2010), underestimates aerosol optical depth (AOD), especially over the area with high AOD (e.g., Asia) when evaluated against 173 AERONET sites globally. Thus, using the same emission inventory, we are likely to underestimate BC concentrations, particularly in Asia, as well. Our simulation follows the standard protocol of the Atmospheric Chemistry and Climate Model Inter-Comparison Project (ACCMIP) and uses standard emission inventories for the year 2000, so that people can inter-compare and evaluate their simulated air quality and climate impacts. In addition to the actual BC simulated by AM3 that represents BC emissions from all regions and sources, we added tagged BC tracers representing anthropogenic BC emitted from four heavily-populated industrial regions (East Asia, South Asia, North America and Europe) and three sectors (land transportation, residential, and industry) in East Asia and South Asia to identify their effects on receptors (including the source regions listed above and the rest of the world, Fig. 1). Our analyses aim to identify regions and sectors where mitigation of anthropogenic BC emissions yields the greatest benefits.

2. Method

2.1. Model description

The global AM3 model is developed by the Geophysical Fluid Dynamics Laboratory (GFDL)/NOAA as the atmospheric component of their coupled general circulation model (CM3). AM3 is designed to address key emerging issues in climate science, including aerosol-cloud interactions and chemistry-climate feedbacks, and has been widely applied in many recent studies (Fang et al., 2013; Lamarque et al., 2013a, 2013b; Lee et al., 2013; Naik et al., 2013; Parrish et al., 2014; Schnell et al., 2015; Shen et al., 2017; Shindell et al., 2013; Silva et al., 2013; Stevenson et al., 2013; Voulgarakis et al., 2013; Young et al., 2013). A finite-volume dynamical core with a cubed-sphere horizontal grid is used (2° latitude × 2.5° longitude), with horizontal resolution varying from 163 km (at the corners of each face) to 231 km (near the center of each face). Vertically, AM3 extends from the surface up to 0.01 hpa (~86 km) with 48 vertical hybrid sigma pressure levels. Vertical resolution ranges from 70 m near the earth's surface to 1–1.5 km near the tropopause and 3–4 km in much of the stratosphere (Donner et al., 2011). The model includes interactive tropospheric and stratospheric chemistry (85 species, including BC) and uses emissions (both natural and anthropogenic) to drive its chemistry and aerosol simulations.

To improve agreement between the simulated lifetime and concentrations of BC with recent observations, a BC aging scheme with updated parameters for estimating BC dry and wet deposition is implemented (Liu et al., 2011; Zhang et al., 2015a). This improved BC aging scheme considers the conversion of hydrophobic BC to hydrophilic BC, as well as the mixing of BC with other aerosols (e.g., sulfate) via characterizing the lifetime of BC with being proportional to OH radical concentrations parameterized according to observations (Liu et al., 2011; Shen et al., 2017). In terms of wet deposition, AM3 includes in-cloud and below-cloud scavenging by large-scale and convective clouds. The wet deposition flux is directly proportional to the local concentration. In-cloud scavenging of aerosols is calculated following the work of Giorgi and Chameides (1985). In the case of convective clouds, wet deposition is only computed within the updraft plume. Below-cloud washout is only considered for large-scale precipitation and is parameterized as by Li et al. (2008) for aerosols. AM3 assumes that both snow and rain have the same scavenging factor and also implements “limiters” to enforce monotonicity and positive definiteness in the tracer mixing ratio profiles, which was later found to cause less effective convective removal than realistic (Paulot et al., 2016; Zhao et al., 2018). Despite the simplicity of the wet deposition scheme, AM3 generally provides a reasonable simulation of the global mean and regional patterns of aerosol optical depth (AOD) (Donner et al., 2011) and of the spatial patterns in surface $PM_{2.5}$ (Fang et al., 2013).

Earlier studies have extensively evaluated the physical (e.g., optical characteristics of aerosols) and chemical (O_3 and $PM_{2.5}$ concentrations) parameters of atmospheric tracers in AM3 (Donner et al., 2011; Fang et al., 2013; Naik et al., 2013). AM3 has also been used in BC study and shown good comparison with other similar models (Liu et al., 2011; Shen et al., 2017; Lee et al., 2013). Liu et al. (2011) found that AM3 has better performance in simulating BC concentrations in the Arctic than all HTAP models considered by Shindell et al. (2008). They also found that AM3 would be among the best models evaluated by Koch et al. (2009). Shen et al. (2017) found that AM3 simulation results for BC in the Arctic compares well to the models in the Arctic Monitoring and Assessment Programme (AMAP), which causes an average underestimation of a factor of 2 for BC at Alert and Barrow.

For this work, we chose AM3, a global chemistry-climate model because: 1) it allows us to conduct a complete and integrated assessment of the BC impacts, not only on air quality, health and glacial deposition as discussed in this paper, but also on the climate (in a parallel project); 2) it enables us to evaluate inter-regional and intercontinental transport of BC and its impacts during average conditions of climate and air quality around the year 2000 (e.g., 1996–2005, a specific time slice on which the Atmospheric Chemistry and Climate Model Inter-Comparison Project -ACCMIP project focused), and thus are comparable to the ACCMIP results; 3) its BC simulation has been earlier assessed to be among the best of similar global chemistry-climate models.

2.2. Tagging BC from various regional and sectoral sources

In addition to the 85 atmospheric chemical species included in the standard AM3 model, we add “tagged” BC species to the model to identify the original source of BC affecting air quality, premature mortality and glacier deposition. Tagged BC species undergo all the dynamical, physical and chemical processes as the untagged BC, but only originate from specific sources and do not affect the simulated climate. Using this method, Liu et al. (2009b) found that the differences between the sum of non-reactive tagged tracers and the concentrations of the same untagged species are less than 1% at most locations thus justifying the use of tagging method for source attribution analyses.

Thus, total BC emissions in this study include BC emissions from all anthropogenic (land anthropogenic, aviation, and shipping) and natural sources. On top of that, we also tag BC from land anthropogenic sources because they can be more manageable and collectively represent 66% of global land anthropogenic and biomass burning BC emissions. To balance tracking specific emissions with computational capacity, we add tagged BC tracers only from four highly-populated source regions (East Asia, South Asia, Europe, and North America (see Fig. 1), which contribute 18%, 7%, 6%, and 5% to global land anthropogenic and biomass burning BC emissions, respectively) and sector-specific tracers from the three largest emission sectors (land transportation, residential, and industry) from East Asia and South Asia.

Our tagged BC species include BC_EA_Trans, BC_EA_Res, BC_EA_Ind, BC_EA_Anthro, BC_SA_Trans, BC_SA_Res, BC_SA_Ind, BC_SA_Anthro, BC_EU_Anthro, and BC_NA_Anthro. Here, ‘EA’, ‘SA’, ‘EU’ and ‘NA’, refer to BC originating from East Asia, South Asia, Europe and North America, respectively. ‘Trans’, ‘Res’, and ‘Ind’ refer to land transportation, residential, and industrial sectors, respectively. Our tagged

transportation BC emissions only include BC from land transport. BC emissions from maritime transport (international shipping, domestic shipping and fishing) and aviation are included in our global total BC emissions (Lamarque et al., 2010), but are not tagged. Residential sector includes emissions from both fossil fuel and biofuel combustion. Also, industrial sector includes emissions from both combustion (including the power sector) and non-combustion industrial processes (Lamarque et al., 2010). "Anthro" is the sum of land anthropogenic emissions from these three sectors (including both fossil fuel and biofuel combustion) and from agricultural waste burning (not including forest or grassland fires) and waste management. Taking the difference between the total contribution of regional anthropogenic BC (e.g., BC_EA_Anthro) and tagged sectoral anthropogenic BC (e.g., BC_EA_Trans, BC_EA_Res, BC_EA_Ind) in the region, we can identify the remaining contribution of other anthropogenic BC emissions in that region. Total BC emissions in the standard AM3 model and these tagged BC species together allow us to quantify the contributions of both total BC emissions and specific anthropogenic BC sources (regional and sectoral) to surface BC concentrations, the premature mortalities resulting from exposure to each source of BC, and BC depositions on glaciers.

2.3. Estimating premature mortality

Some studies suggest that combustion-related particulate matter (including BC) is more toxic than other $PM_{2.5}$ components and that BC itself may act as a "universal carrier" of toxic particles (Cooke et al., 2007; Grahame and Schlesinger, 2007; Hoek et al., 2013; Morton et al., 2013; REVIHAAP, 2013). However, while efforts are growing to isolate the specific health effects of different components of fine particles ($PM_{2.5}$), evidence for differential toxicity is not fully conclusive (EPA, 2009; Janssen et al., 2012; REVIHAAP, 2013). Therefore, we treat BC as a fractional component of $PM_{2.5}$ to estimate BC associated premature mortality in the main analysis. Specifically, we use the $PM_{2.5}$ relative risk (RR) functions for adults (≥25 years old) from Burnett et al. (2014) for ischemic heart disease (IHD), cerebrovascular disease (stroke), chronic obstructive pulmonary disease (COPD), and lung cancer (LC), as their study covers the global range of $PM_{2.5}$ exposures, using the equation below. Burnett et al. (2014) provides concave-shaped disease-specific integrated exposure–response (IER) functions to capture the variations in premature deaths due to changes in $PM_{2.5}$ exposures. Details for the disease-specific IER functions can be found in Fig. 1 in Burnett et al. (2014) and the Global Burden of Disease Study 2010) - Ambient Air Pollution Risk Model 1990–2010 database (http://ghdx.healthdata.org/record/global-burden-disease-study-2010-gbd-2010-ambient-air-pollution-risk-model-1990-2010).

$$\Delta Mort_i = POP_{25} * MortBase_i * \left[1 - \frac{RR_i(C_{PM2.5-BC_s})}{RR_i(C_{PM2.5})}\right] \quad (1)$$

In each AM3 model grid cell, we estimate BC_s associated premature mortality from disease i ($\Delta Mort_i$) based on the adult population aged 25 and older (POP_{25}), the baseline mortality rate in adults for disease i ($MortBase_i$), the relative risk for disease i (RR_i) at the simulated total surface $PM_{2.5}$ concentrations ($C_{PM2.5}$), and the relative risk for disease i at the $PM_{2.5}$ concentrations without the contribution of the specific BC source ($C_{PM2.5-BC_s}$). BC_s refers to individual BC species, either the total untagged BC (total BC surface concentrations are obtained from standard AM3 runs) or each of our tagged regional or sectoral BC tracers. We obtain the 2000 global population data at 1 km^2 grid level from CIESIN (2005). Country-level age distribution and baseline mortality rates for IHD, stroke, COPD, and LC for the year 2000 are from the GBD project (http://www.healthdata.org/gbd) and are assumed uniform within each country.

In our main analysis, we assume equal toxicity between undifferentiated $PM_{2.5}$ and BC. In order to test the sensitivity of our estimated BC associated health impacts to this assumption, we also estimate health impacts using BC-specific exposure-response functions for all-cause mortality from a meta-analysis by Hoek et al. (2013). Unlike the concave integrated exposure-response functions of Burnett et al. (2014), the BC-specific functions are (log-) linear. Therefore, for comparison, we also include a second sensitivity study using a recently-updated (log-) linear exposure-response function for all-cause mortality for undifferentiated $PM_{2.5}$ (Forestiere et al., 2014). Details of the sensitivity studies are reported in the SI.

2.4. Calculating attribution efficiency

To identify regions and sectors that impose the largest negative environmental impacts from each unit of BC emission, we estimate the BC attribution efficiency for air quality, premature mortality, and glacial deposition. The "attribution efficiency" for BC surface concentrations, BC associated premature mortality, or BC deposited to glaciers is defined as the magnitude of BC concentrations (μg/m^3), the number of premature deaths (cases), or the amount of BC deposition (μg/m^2/day) in receptor regions resulting from each Gg of BC emitted from a specific source region or sector ($AE_{r-s,k} = \frac{I_{r-s,k}}{E_s}$), respectively. $AE_{r-s,k}$ is the attribution efficiency for a specific type of environmental impact k (e.g., BC associated premature mortality) in receptor region r due to tagged BC tracer from source s, $I_{r-s,k}$ is the environmental impact k in receptor region r due to tagged BC tracer from source s, E_s is the emission of source s. A high attribution efficiency for a specific BC tracer indicates that a unit reduction from that source will likely result in a relatively large reduction in the negative environmental impact at the receptor region.

3. Results

3.1. Regional and sectoral attribution of annual average simulated BC surface concentrations

We evaluate the effect of total global BC emissions and emissions originating from each of our tagged regions and sectors on simulated annual average surface BC concentrations. Simulated global annual average BC surface concentrations exhibit hotspots in Asia, particularly in eastern China and the Indo-Gangetic plain of India (Fig. 2), with the highest concentrations found in Shandong province in China (~3.5 μg/m^3). BC surface concentrations in Europe and the United States are much lower - roughly 0.05–1 μg/m^3 and 0.05–0.5 μg/m^3, respectively. BC emissions from each of our four tagged regions are primarily concentrated within their respective source regions (Fig. 2).

We also present the simulated annual average population-weighted (P-W) BC surface concentrations ($C_{PW}(R) = \frac{\sum_{i=1}^{n} Pop_i(R) * C_i(R)}{\sum_{i=1}^{n} Pop_i(R)}$) in the four tagged regions in Fig. 3. $C_{PW}(R)$ refers to P-W annual average BC surface concentrations in each tagged region R, Pop_i refers to population in grid i, and $C_i(R)$ refers to model simulated BC concentrations in grid i in region R. As shown in Fig. 3, East Asia (1.7 μg/m^3) and South Asia (1.1 μg/m^3), the two regions with the largest population, also have the highest P-W concentrations, followed by Europe (0.5 μg/m^3) and North America (0.4 μg/m^3). We find that domestic anthropogenic BC emissions dominate that region's P-W BC surface concentrations, accounting for 96%, 93%, 89% and 93% of surface BC concentrations over East Asia, South Asia, Europe and North America, respectively. Any individual foreign contributions to P-W BC concentrations are generally below 1%. Within each region, the sectors that contribute most to domestic P-W BC concentrations are the industrial sector in East Asia (~50%) and the residential sector in South Asia (~60%). We find that in East Asia and South Asia, sectoral contributions to P-W BC surface concentrations are roughly proportional to their domestic emission shares.

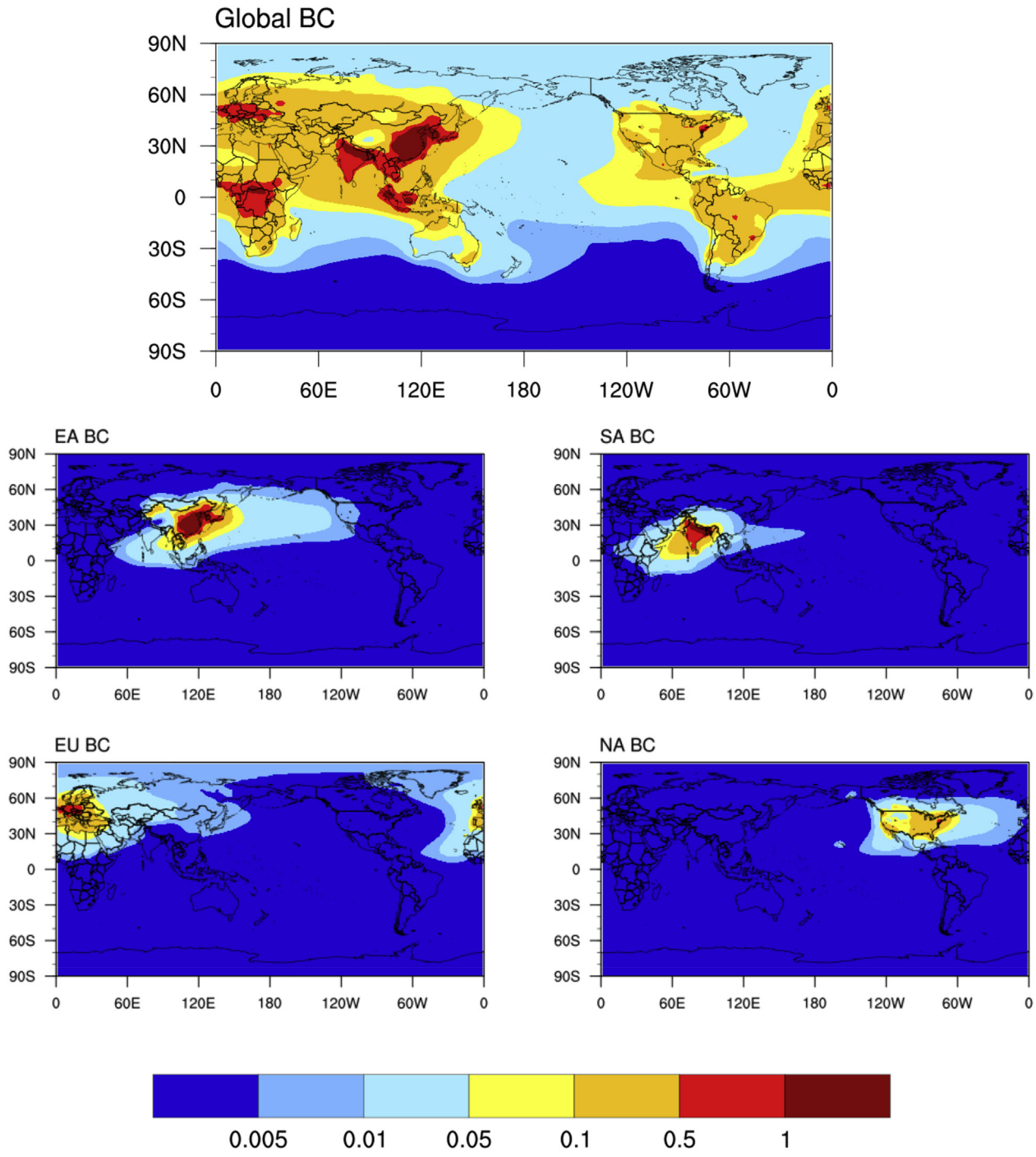

Fig. 2. Annual average BC surface concentrations (μg/m^3) resulting from global total BC emissions, and land anthropogenic BC emissions from each tagged region in 2000: East Asia (EA), South Asia (SA), Europe (EU), and North America (NA).

3.2. Regional and sectoral attribution of BC associated premature mortality

We estimate global total BC associated premature mortality to be 106,000 annually (95% confidence interval, CI, 45,000–143,000, see Table 1 and Supplementary Fig. S1), with ranges reflecting the low and high estimates of relative risks for $PM_{2.5}$ exposure reported in Burnett et al. (2014). Globally, we estimate 2.1 million (95% CI, 1.0–3.1 million) $PM_{2.5}$ associated premature deaths, which is roughly 20 times that of our estimated BC associated premature deaths. Our estimated $PM_{2.5}$ associated premature mortality is comparable to earlier studies. For instance, Silva et al. (2013) estimated 2.1 million (95% CI, 1.3–3.0 million) global premature deaths due to $PM_{2.5}$. As shown in Fig. 4 and Fig. S2, high BC associated premature mortality primarily occurs in East Asia (over 10 BC associated premature deaths/1000 km^2 in eastern China) and South Asia (1–10 BC associated premature deaths/1000 km^2 across India), both regions with high BC concentrations and dense population. Accordingly, approximately half of the global total BC associated premature deaths occur in East Asia, followed by 17% in South Asia. In contrast, BC associated premature mortality is relatively low in Europe (0.1–10 premature deaths/1000 km^2) and North America (0.1–1 premature deaths/1000 km^2 in eastern U.S.), contributing approximately 12% and 4% of the global total BC associated premature deaths, respectively.

We further quantify the source attribution of regional and sectoral

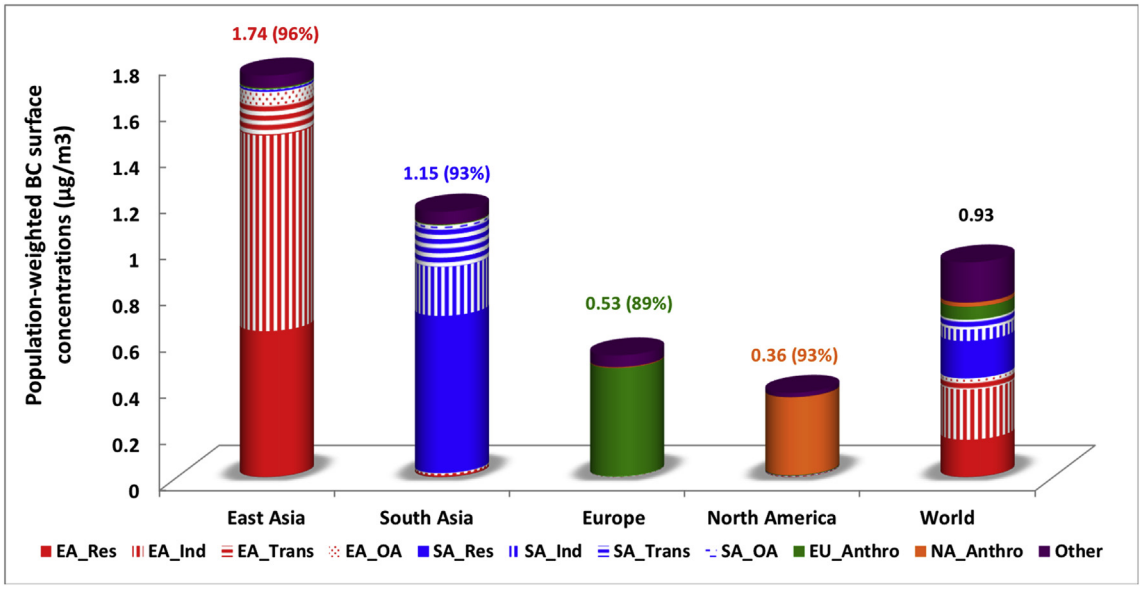

Fig. 3. Annual average population-weighted BC surface concentrations in receptor regions (µg/m^3). Percentages in parentheses represent the intra-regional contribution to annual average BC concentrations in the surface layer over each receptor region. EA, SA, EU, and NA refer to regions defined in Fig. 1a. Res, Ind, Trans, OA, and Anthro refer to the residential, industrial, and land transportation sectors plus other land anthropogenic sources (e.g., agricultural waste burning and waste management), and total land anthropogenic BC emissions, respectively. Other emissions include untagged anthropogenic emissions and biomass burning emissions.

BC emissions on BC associated premature mortality (Table 1). In each region, emissions from that region (domestic emissions) generally account for over 90% of total BC associated premature mortality while the contribution from any given foreign region is typically below 1%. From the sectoral perspective, domestic BC emissions from the industrial (~50%) and residential (~35%) sectors make up ~85% of BC associated premature deaths occurring in East Asia. The residential sector dominates (~60%) BC associated premature deaths in South Asia. Similar to BC surface concentrations, in both East Asia and South Asia, sectoral contributions to BC associated premature mortality are roughly

Table 1
Annual average premature mortality associated with BC exposure in each receptor region resulting from specific regional and sectoral sources (unit: deaths).

Sources		Receptors				
		EA	SA	EU	NA	World
Total BC		51,500 (15,600–69,400)	17,600 (8000–27,900)	12,300 (7300–15,500)	4400 (2800–4700)	106,100 (44,900–143,400)
EA_Anthro		48,900 (95%) (14,800–65,700)	310 (2%) (96–506)	32 (0.3%) (20–42)	46 (1%) (25–65)	50,100 (47%) (15,300–67,500)
	EA_Trans	3800 (7%) (1500–5000)	30 (0.2%) (9–48)	4 (0.0%) (3–5)	6 (0.1%) (3–8)	3900 (4%) (1500–5300)
	EA_Res	18,100 (35%) (5300–24,300)	120 (0.7%) (36–190)	11 (0.1%) (7–14)	16 (0.4%) (8–22)	18,500 (17%) (5500–25,000)
	EA_Ind	24,200 (47%) (7100–33,000)	160 (0.9%) (49–255)	16 (0.1%) (10–21)	23 (0.5%) (12–32)	24,700 (23%) (7400–33,800)
SA_Anthro		380 (0.7%) (129–616)	16,100 (92%) (7200–25,800)	11 (0.1%) (7–16)	14 (0.3%) (8–19)	16,800 (16%) (7500–26,800)
	SA_Trans	65 (0.1%) (21–97)	2600 (15%) (800–3900)	2 (0.0%) (1–3)	2 (0.1%) (1–3)	2700 (3%) (840–4100)
	SA_Res	240 (0.5%) (80–390)	10,400 (59%) (4100–16,300)	7 (0.1%) (4–10)	9 (0.2%) (5–12)	10,800 (10%) (4300–17,000)
	SA_Ind	75 (0.1%) (25–115)	3200 (18%) (1000–5000)	2 (0.0%) (1–3)	3 (0.1%) (2–4)	3400 (3%) (1100–5300)
EU_Anthro		170 (0.3%) (62–215)	55 (0.3%) (19–81)	11,000 (89%) (6500–13,800)	18 (0.4%) (12–22)	13,100 (12%) (7700–16,000)
NA_Anthro		31 (0.1%) (11–40)	14 (0.1%) (5–21)	81 (0.7%) (50–103)	4100 (93%) (2600–4300)	4300 (4%) (2700–4600)

Total BC includes emissions from all anthropogenic (land anthropogenic, aviation, and shipping) and natural sources as included in the standard AM3 model. EA, SA, EU and NA refer to tagged BC emissions from East Asia, South Asia, Europe and North America, respectively. Trans, Res and Ind refer to tagged BC emissions from land transportation, residential and industrial sectors, respectively. Anthro refer to the sum of land anthropogenic BC emissions (Trans + Res + Ind + additional anthropogenic sources) in each tagged region.

BC surface concentrations due to total BC emissions are obtained from the untagged standard AM3 model output for BC. Regional premature deaths due to total BC emissions are obtained by summing up grid-level premature deaths (calculated via Eq. (1)) occurring in each region due to total BC emissions. For instance, total BC emissions cause 51,500 premature mortalities in East Asia.

Percentages shown in this table refer to the contributions of BC emissions from each source region and sector to total premature deaths in the receptor region (e.g., EA total land anthropogenic BC emissions are responsible for 95% of total premature mortality in East Asia associated with global total BC emissions).

Number ranges shown in this table refer to the lower and upper bound estimates in BC associated premature deaths due to uncertainties in $PM_{2.5}$ relative risks.

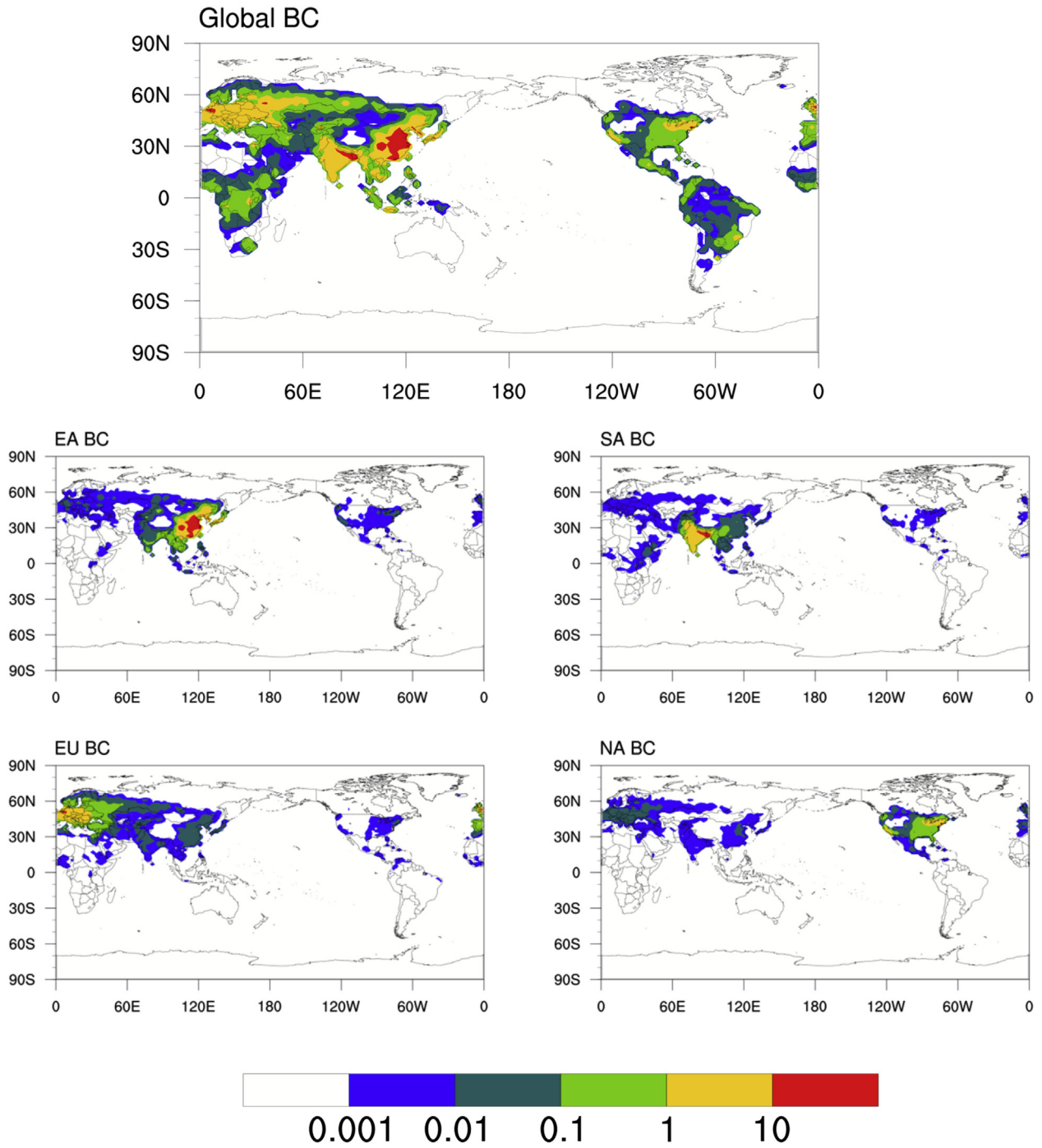

Fig. 4. Premature mortality (deaths per 1000 km^2) associated with global total BC emissions, and land anthropogenic BC emissions from each tagged region in 2000: East Asia (EA), South Asia (SA), Europe (EU), and North America (NA).

proportional to their respective emission shares.

Our sensitivity analyses (Fig. S1) demonstrate that our calculated health impacts from BC exposure would be much higher if BC toxicity is greater than that of typical $PM_{2.5}$. We find that using log-linear BC-specific relative risks (Fig. S1b) leads to a mortality burden that is about 10 times higher than what we obtain with the log-linear $PM_{2.5}$ concentration-response functions (Fig. S1c). In comparison, the differences in estimated premature mortality between the cause-specific, concave $PM_{2.5}$ concentration-response functions (Fig. S1a) and the log-linear $PM_{2.5}$ concentration-response functions (Fig. S1c) are much smaller (generally within 3 times). Therefore, only a relatively small part of the difference is attributable to assumptions about the shape of the exposure-response relationship (log-linear versus concave) and the number of causes (all causes versus four causes) (Fig. S1). The primary difference results from the difference in toxicity of different $PM_{2.5}$ components. This indicates that our main estimates of the mortality burden associated with BC exposure, which are based on changes to total $PM_{2.5}$ concentrations, are conservative should evidence of enhanced toxicity of BC be confirmed.

3.3. Regional and sectoral attribution of BC deposition on northern hemispheric glaciers

We analyze BC deposition at the specific locations of individual

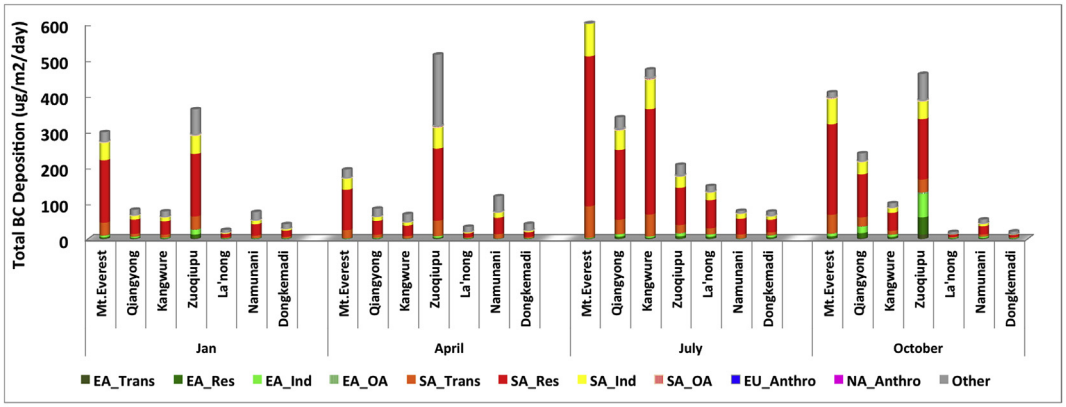

(a)

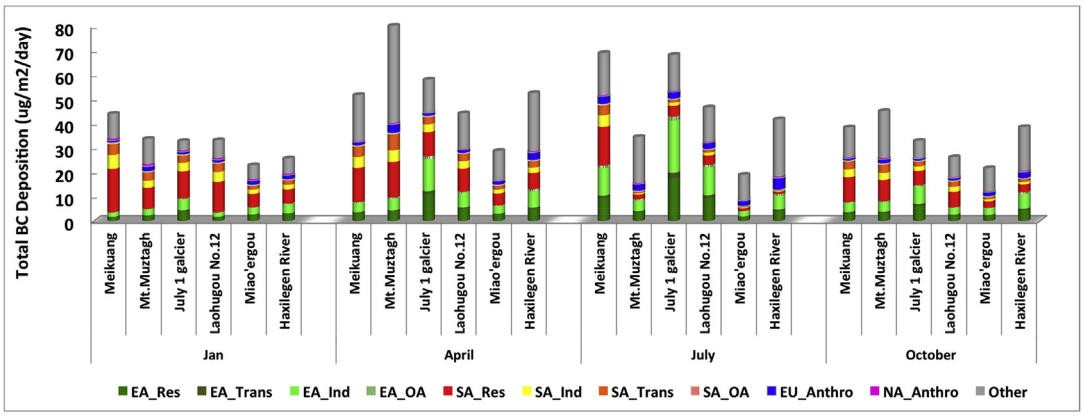

(b)

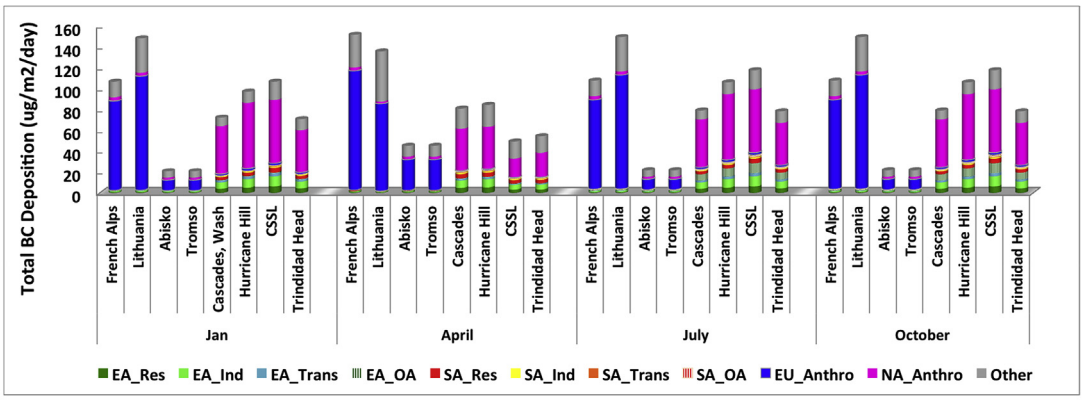

(c)

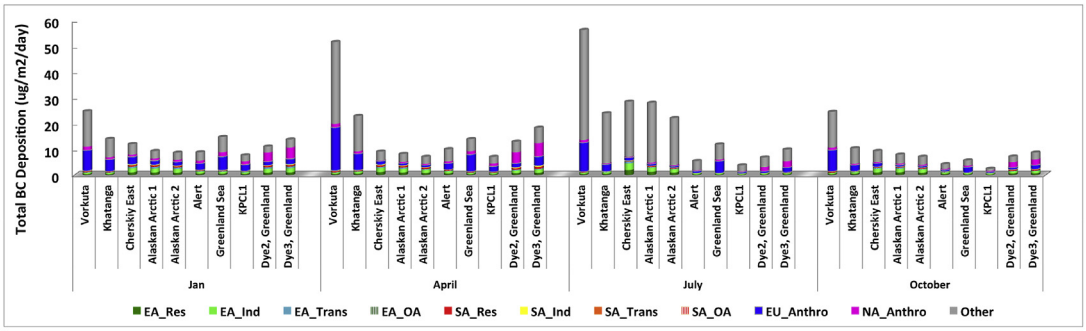

(d)

Fig. 5. Total BC deposition on glaciers (μg/m^2/day) in (a) Southern and Central Himalayas and Tibetan Plateau (HTP), (b) northern HTP, (c) Europe and North America, and (d) Arctic. Arctic glaciers located in northwestern Russia (Vorkuta), north central Russia (Khatanga), northeastern Russia (Cherskiy East), Alaska (Alaskan Arctic 1 and 2), northern Greenland (Alert, Greenland Sea, KPL1), and southern Greenland (Dye2 and Dye3). See Fig. S3 and Table S1 for glacier locations.

glaciers in each region. Detailed geographic information of glaciers evaluated are shown in Fig. S3 and Table S1. Due to notable spatial heterogeneities and seasonal variations for BC deposition, we quantify the seasonal contributions of regional and sectoral anthropogenic BC emissions to BC deposition on glaciers in Asia, Europe, North America and the Arctic, respectively (Fig. S4).

3.3.1. Asia glaciers

In Asia, we focus on the Himalayan Tibetan Plateau (HTP) glaciers. For nearly all these glaciers, seasonal contributions of land anthropogenic BC from South Asia and East Asia represent between ~40% and 95% of total BC deposition. Southern Tibetan glaciers receive a relatively large total BC deposition (Fig. 5a). On these glaciers, South Asian land anthropogenic BC emissions alone account for ~60–90% of total BC deposition across seasons, of which ~40–60% is attributed to the residential sector. This is consistent with earlier findings that South Asia is the major source of BC in southern HTP (Zhang et al., 2015b). Besides, due to the Asian monsoon that carries emissions from South Asia northwards, these glaciers usually have the largest total deposition in summer, when South Asian emissions account for 80–90% of total BC deposition (Fig. 5a). In contrast, the largest East Asian contribution to BC deposition on these glaciers occurs in October (e.g., ~30% in Zuoqiupu), in part because of the returning winter monsoonal flow. In other seasons, East Asia contributes less than 10% of total BC deposition. Regional contributions to BC deposition on central and southern HTP glaciers are similar, though total deposition on central HTP glaciers is much lower than on southern HTP glaciers (Fig. 5a). In the northern Tibetan Plateau, we generally find a dominant East Asian contribution in summer among our tagged tracers, which has also been identified in previous studies (Li et al., 2016; Zhang et al., 2015b). However, our study finds that south Asian land anthropogenic BC emissions mostly dominate BC deposition in the northern Tibetan Plateau in other seasons, though East Asian emissions are also important (Fig. 5b). Additionally, European land anthropogenic BC emissions deposit 1–10% of total BC on northern Tibetan glaciers, particularly on Haxilegen River and Mt. Muztagh glaciers, with the largest contributions in summer. Kopacz et al. (2011) identify a strong snow-albedo driven seasonal cycle (lowest in winter and highest in summer) in radiative forcing on northern Tibetan glaciers, indicating an enhancement of potential glacial melting due to glacial deposition of BC in summer. Thus, East Asian land anthropogenic BC emissions, which contribute most to northern HTP glacial deposition in summer, are likely to enhance northern HTP glacial melting most.

3.3.2. European and North American glaciers

As shown in Fig. 5c, anthropogenic BC emissions within each source region dominate BC deposition over both European and North American glaciers in all seasons. For European glaciers, domestic land anthropogenic BC emissions contribute ~50–90% of total BC deposition, depending on the season. In comparison, contributions from East Asia, South Asia and North America are each generally below 5%, with the remaining originating from either wildfires or BC emission sources outside the tagged regions.

Similarly, North American land anthropogenic BC emissions contribute ~40–80% of BC deposition on North American glaciers. Notably, East Asian land anthropogenic BC emissions contribute ~20% to BC deposition on western US glaciers (e.g., Washington state and the Sierra Nevada mountains) during non-summer seasons, with roughly 9% and 7% attributable to the East Asian industrial and residential sectors, respectively.

3.3.3. Arctic glaciers

BC deposition on Arctic glaciers is of particular concern due to their critical role in affecting the climate via positive feedbacks on melting sea ice (McConnell et al., 2007; Ramanathan and Carmichael, 2008). We find that European (~25%), East Asian (~13%), North American (~7%), and South Asian (~3%) land anthropogenic emissions together contribute about half of annual average total BC deposition to the Arctic (> 67° N), though large variations exist depending on the geographic location of glaciers and the season (Fig. 5d and Fig. S4). The other half of BC deposition over the Arctic may come from emissions from biomass burning (wildfires) and other untagged sources. For example, BC from biomass burning has been found to make up 40% of BC in Arctic air (Winiger et al., 2016), and to account for over 90% of BC in Arctic snow when counted along with biofuel (Hegg et al., 2009).

Fig. 5d shows the seasonal contributions of our tagged anthropogenic BC emissions to BC deposition on Arctic glaciers in Alaska, Greenland, and Russia. Our tagged anthropogenic BC emissions from four tagged regions together explain roughly 60–80% of the total BC deposition on Alaskan and Greenland glaciers and about 40%–60% on Russian glaciers in non-summer seasons. The lower contribution of tagged emissions on Russian glaciers suggests that untagged Russian emissions (particularly domestic biomass burning may contribute roughly half of total Russian BC emissions) are an important source of BC deposition (Lamarque et al., 2010). Contributions from untagged wildfire emissions are particularly notable in summer, when our tagged anthropogenic BC emissions together only explain ~20%, ~45%, and ~25% of total BC deposition over Alaska, Greenland, and Russian glaciers. This is most likely due to large contributions to Arctic BC from European and Siberian boreal fires in summer (Bond et al., 2013; Hegg et al., 2009; McConnell et al., 2007).

In our simulations, Alaskan glaciers, depending on the season, receive ~10–35% of their total BC deposition from East Asian land anthropogenic BC emissions, significantly more than from Europe (~3–20%), North America (~2–10%) or South Asia (~1–5%). For southern Greenland glaciers (e.g., Dye2), North American land anthropogenic BC emissions, depending on the season, contribute ~20–30% of BC deposition, followed by Europe with ~10–20%. In comparison, among our tagged emissions, European land anthropogenic BC emissions dominate BC deposition onto northern Greenland glaciers (~20–50% depending on the season). We also find that of our tagged emissions, European and East Asian land anthropogenic BC emissions dominate BC deposition over western and eastern Russian glaciers, respectively.

3.4. Attribution efficiency of BC impacts on air quality, premature mortality, and deposition on glaciers

We estimate the attribution efficiency for annual average P-W BC concentrations, BC associated premature mortality, and BC deposition on glaciers (Supplementary Tables S2- S4).

As shown in Supplementary Table S2, across regions, each unit of BC emission in South Asia contributes the most (ie. has the largest attribution efficiency) to BC surface concentrations within its own source region (approximately 60%, 80%, and 95% higher than attribution efficiency in East Asia, Europe, and North America, respectively). This is primarily because the annual average lifetime of BC from South Asia is longer than from other regions mainly due to less efficient wet deposition (Shindell et al., 2008). In comparison, East Asia has the largest attribution efficiency in BC-associated premature deaths within its own source region, roughly 35 (11–47) premature deaths per Gg BC. In comparison, South Asia, Europe, and North America have attribution efficiencies of 28 (13–45), 25 (15–31) and 12 (7–12) premature deaths per Gg BC of their own emissions, respectively (Supplementary Table S3). Ranges of premature mortality attribution efficiency are due to uncertainties in the $PM_{2.5}$ relative risks. Higher attribution efficiency for BC associated premature mortality in East Asia primarily occurs because the adult population in East Asia was ~1.5, ~2.2, and ~4.2 times higher than in South Asia, Europe, and North America in the year 2000, respectively. Nevertheless, the number of adults in India has grown rapidly since 2000

(http://esa.un.org/unpd/wpp/Download/Standard/Population/),

and is estimated to surpass China around 2040 (Fig. S5). Thus, the attribution efficiency for BC associated premature mortality will likely increase in South Asia.

We find that South Asian emissions have the largest BC deposition attribution efficiency over Asian glaciers (Table S4). Specifically, in southern and central (northern) Tibetan glaciers, each unit of South Asian emissions results in 10–100 times (1–4 times) more BC deposition than the same quantity of East Asian emissions. Similarly, for European and North American glaciers, domestic BC emissions have 1–2 orders of magnitude larger attribution efficiencies for BC deposition than BC emissions from any foreign region. Notably, for most Arctic glaciers, anthropogenic BC emissions from Europe generally have the largest BC deposition attribution efficiency among our tagged tracers. However, the largest attribution efficiency for southern Greenland glaciers is from North America.

Sectoral differences affecting the attribution efficiency of BC concentrations, premature mortality, and deposition on glaciers are generally small. However, our estimated premature mortality attributed to emissions from the residential sector does not account for indoor air pollution, which resulted in over 3 million premature deaths worldwide in 2000 (http://www.healthdata.org/gbd). Thus, including the effects of indoor air pollution would substantially increase the attribution efficiency of total (indoor plus outdoor) BC associated premature mortality associated with the residential sector.

4. Discussion

To evaluate the potential benefits of various BC mitigation strategies, this study systematically quantifies the source attribution of regional and sectoral BC emissions on air quality, premature mortality and deposition on glaciers by tagging land anthropogenic BC tracers from four regions and three sectors within a global coupled chemistry-climate model.

We find that intra-regional emissions usually contribute over 90% of BC surface concentrations and associated premature mortality, as well as ~40–95% of BC deposition on glaciers within each region. Additionally, domestic BC emissions generally contribute approximately 1–2 orders of magnitude more to BC concentrations, associated premature deaths, and BC deposition on glaciers than the same quantity of foreign emissions. This indicates that reducing domestic BC emissions can bring both the largest total reduction potential and the highest reduction efficiency for the BC associated environmental impacts we evaluate in this work.

Across regions, people in East Asia and South Asia are exposed to the highest BC surface concentrations and suffer from the largest resulting premature mortality. Among the 106,000 (95% CI: 45,000–143,000) cases of BC associated premature deaths globally, ~70% occur in Asia. Within either East Asia or South Asia, sectoral contributions to BC surface concentrations and associated premature mortality, and to BC deposition on glaciers are roughly proportional to their emission shares. For instance, the South Asian residential sector, which accounts for approximately 60% of total regional land anthropogenic BC emissions, contributes ~60% of domestic population-weighted (P-W) BC concentrations and associated premature mortality, as well as ~40–60% of total BC deposition on southern Tibetan glaciers.

Regarding attribution efficiency, the largest attribution efficiency for health impacts occurs in East Asia, where it is approximately 20%, 40%, and 200% larger than in South Asia, Europe, and North America, respectively, primarily due to the co-location of dense population and high BC emissions in East Asia. Importantly, the health impacts from each unit of BC emission have increased significantly in South Asia over the past decade due to rapid population growth. Sectoral differences in attribution efficiency for BC associated premature mortality from outdoor air pollution are usually small. However, BC emission from the residential sector may be particularly important given the adverse impacts of indoor air pollution and associated health burden (Smith and Mehta, 2003). Overall, this implies that BC mitigation may be particularly beneficial in Asia, especially from the residential sector.

Although domestic BC dominates regional impacts, foreign contributions to premature mortality and BC deposition on glaciers do occur, particularly for regions with little domestic BC emission sources. For instance, East Asian anthropogenic BC emissions are a large contributor to BC deposition over the Arctic, especially on Alaskan glaciers (~10–35% across seasons). Thus, even though the Arctic countries can work together through the Arctic Council to mitigate emissions of their own short-lived climate forcers (Sand et al., 2016), our study suggests it would be beneficial for them to facilitate East Asian BC emission reductions, particularly for Alaskan glaciers. Over the past decade, international efforts to facilitate BC mitigation in developing countries by institutions such as the Climate and Clean Air Coalition (CCAC, 2012) and Global Alliance for Clean Cookstoves (GACC, 2010) have made some progress at reducing emissions. Continuing international collaboration for existing projects as well as local capacity building, particularly in South Asia and East Asia, will be beneficial to ensure sustainable and cost-effective BC mitigation in these regions, especially in the residential sector (Baron et al., 2015; UNEP, 2011).

We recognize that results in this study are subject to various uncertainties from emission inventories, the representation of BC in our model, and the concentration-response functions used in this study. BC emission inventory studies report large uncertainties (e.g., a factor of 2–4 in Asia) due to challenges in quantifying particle emissions from incomplete combustion and in determining BC emitting activity levels (Bond et al., 2013; Cohen and Wang, 2014; Qin and Xie, 2011a,b; 2012; Zhao et al., 2011). Also, although this version of the AM3 model uses an updated representation of BC aging (Liu et al., 2011; Zhang et al., 2015a), it still does not perfectly capture the chemical-physical transformation of BC. Thus, better quantification of the BC emission inventory and model development advances will be valuable in improving BC source attribution estimates. Our study identifies substantial uncertainties in BC associated health impacts due to different concentration-response functions. In addition, recent studies identified higher $PM_{2.5}$ concentration-responses than the Burnett et al. (2014) results (Heft-Neal et al., 2018). As our simulated BC concentrations from the global coarse-resolution chemistry-climate model tend to underestimate BC concentrations especially in urban areas (Lamarque et al., 2010), and latest studies find larger exposure–responses than Burnett et al. (2014), our estimated BC associated premature deaths are conservative. However, such underestimates are unlikely to change our qualitative conclusions in terms of the dominant local benefits of BC mitigation.

Our study focuses on year 2000 to be comparable to ACCMIP results. However, BC emissions have evolved over the past two decades (Bond et al., 2013; Mao et al., 2016; Qin and Xie, 2012). Granier et al. (2011) have made a comprehensive comparison of various bottom-up anthropogenic and biomass burning emission inventories between 1980 and 2010. Their comparison indicates that globally, all emission inventories agree that anthropogenic BC emissions increased from 2000 to 2010 although the rate of increase decreased around 2005. Granier et al. (2011) also found that all emission inventories suggested a strong increase in anthropogenic BC emissions from China and India during this period, though different emission inventories identified either small increases or decreases in anthropogenic BC emissions in Western and Central Europe as well as in the United States. The increasing trend in China and India is consistent with a few later Asian-focused studies. For example, Bond et al. (2013) found that Asian BC emissions increased from ~7.5 Tg/yr in 2000 to 9.8 Tg/yr in 2005. Likewise, Qin and Xie (2012) found that BC emissions in China, the world's largest BC emitter, increased from ~1.2 Tg/yr in 2000 to ~1.9 Tg/yr in 2009. Similar global and regional trends are also captured in the Representative Concentration Pathways (RCP) scenarios. The RCP8.5 has been especially considered to be a reasonable extension of the ACCMIP

simulations beyond 2000 (Granier et al., 2011)). All RCP scenarios also show increases in BC emissions from 2000 to 2010, though they also suggest that total BC emissions peaked in 2010 and will reach a similar emission level to 2000 in 2020 (Fig. S6a). Nevertheless, at the regional level, BC emissions show a consistent increasing trend in Asia from 2000 to 2020, though it has been decreasing in the OECD countries (including Europe and North America) during the same period (Fig. S6b). Meanwhile, global population has increased from ~6 billion in 2000 to ~7 billion in 2015, with particularly large growth in South and East Asia. These region-specific trends in both BC emissions and population growth suggest that the source attribution of south and east Asian BC emissions on air quality, health and glacier deposition is likely to be even more important in more recent years than what we identified in this study. Notably, recent studies also find that BC can further enhance air pollution via modifying boundary layer meteorology (Wang et al., 2018; Ding et al., 2016), which could result in even larger negative health impacts.

To motivate near-term mitigation, our study focuses on immediate benefits including air quality, human health and black carbon deposition on glaciers. However, it would be valuable to have future studies evaluate the radiative effect of black carbon deposition on snowmelt and glacier retreat to better understand the impacts of black carbon on water resources.

Competing interests

The authors declare that they have no competing interests.

Acknowledgement

Y. Qin and Y. Fang thank Princeton University's Woodrow Wilson School of Public and International Affairs for graduate and post-doctoral funding.

Appendix A. Supplementary data

Supplementary data to this article can be found online at https://doi.org/10.1016/j.atmosenv.2019.02.048.

References

Baron, R.E., Montgomery, W.D., Tuladhar, S.D., 2015. An Analysis of Black Carbon Mitigation as A Response to Climate Change. Copenhagen consensus on climate.
Bond, T.C., Doherty, S.J., Fahey, D.W., Forster, P.M., Berntsen, T., DeAngelo, B.J., et al., 2013. Bounding the role of black carbon in the climate system: a scientific assessment. J. Geophys. Res.-Atmos. 118, 5380–5552.
Brandt, J., Silver, J.D., Frohn, L.M., Geels, C., Gross, A., Hansen, A.B., et al., 2012. An integrated model study for Europe and North America using the Danish Eulerian Hemispheric Model with focus on intercontinental transport of air pollution. Atmos. Environ. 53, 156–176.
Burnett, R.T., Pope, C.A., Ezzati, M., Olives, C., Lim, S.S., Mehta, S., et al., 2014. An integrated risk function for estimating the global burden of disease attributable to ambient fine particulate matter exposure. Environ. Health Perspect. 122, 397–403.
CCAC, 2012. The Climate and Clean air Coalition to Reduce Short-Lived Climate Pollutants. http://www.ccacoalition.org/en.
CIESIN, 2005. Center for International Earth Science Information Network, Columbia University; and Centro Internacional de Agricultura Tropical (CIAT), Gridded Population of the World, Version 3 (GPWv3). Socioeconomic Data and Applications Center (SEDAC), Columbia University, Palisades, NY available at: http://sedac.ciesin.columbia.edu/gpw.
Cohen, J.B., Wang, C., 2014. Estimating global black carbon emissions using a top-down Kalman Filter approach. J. Geophys. Res.-Atmos. 119, 307–323.
Cooke, R.M., Wilson, A.M., Tuomisto, J.T., Morales, O., Tainio, M., Evans, J.S., 2007. A Probabilistic characterization of the relationship between fine particulate matter and mortality: elicitation of European experts. Environ. Sci. Technol. 41, 6598–6605.
Ding, A.J., Huang, X., Nie, W., Sun, J.N., Kerminen, V.M., Petaja, T., Su, H., Cheng, Y.F., Yang, X.Q., Wang, M.H., Chi, X.G., Wang, J.P., Virkkula, A., Guo, W.D., Yuan, J., Wang, S.Y., Zhang, R.J., Wu, Y.F., Song, Y., Zhu, T., Zilitinkevich, S., Kulmala, M., Fu, C.B., 2016. Enhanced haze pollution by black carbon in megacities in China. Geophys. Res. Lett. 43, 2873–2879.
Donner, L.J., Wyman, B.L., Hemler, R.S., Horowitz, L.W., Ming, Y., Zhao, M., et al., 2011. The dynamical core, physical parameterizations, and basic simulation characteristics of the atmospheric component AM3 of the GFDL global coupled model CM3. J. Clim. 24, 3484–3519.
EPA, 2012. Report to Congress on Black Carbon. . https://www3.epa.gov/blackcarbon/2012report/Chapter4.pdf.
EPA, 2009. Final Report: Integrated Science Assessment for Particulate Matter. U.S. Environmental Protection Agency, Washington, DC EPA/600/R-08/139F, 2009. (U.S. EPA). 2009.
Fang, Y., Naik, V., Horowitz, L.W., Mauzerall, D.L., 2013. Air pollution and associated human mortality: the role of air pollutant emissions, climate change and methane concentration increases from the preindustrial period to present. Atmos. Chem. Phys. 13, 1377–1394.
Forestiere, F., Kan, H., Cohen, A., 2014. Updated Exposure-Response Functions Available for Estimating Mortality Impacts.
GACC, 2010. Global Alliance for Clean Cookstoves. http://cleancookstoves.org.
Giorgi, F., Chameides, W.L., 1985. The rainout parameterization in a photochemical model. J. Geophys. Res.-Atmos. 90, 7872–7880.
Grahame, T.J., Schlesinger, R.B., 2007. Health effects of airborne particulate matter: do we know enough to consider regulating specific particle types or sources? Inhal. Toxicol. 19, 457–481.
Granier, C., Bessagnet, B., Bond, T., D'Angiola, A., van der Gon, H.D., Frost, G.J., et al., 2011. Evolution of anthropogenic and biomass burning emissions of air pollutants at global and regional scales during the 1980-2010 period. Clim. Change 109, 163–190.
Heft-Neal, S., Burney, J., Bendavid, E., Burke, M., 2018. Robust relationship between air quality and infant mortality in Africa. Nature 559, 254–258.
Hansen, J., Nazarenko, L., 2004. Soot climate forcing via snow and ice albedos. In: Proceedings of the National Academy of Sciences of the United States of America. vol. 101. pp. 423–428.
Huang, X., Song, Y., Zhao, C., Cai, X.H., Zhang, H.S., Zhu, T., 2015. Direct radiative effect by multicomponent aerosol over China. J. Clim. 28, 3472–3495.
Huang, X., Wang, Z.L., Ding, A.J., 2018. Impact of aerosol-PBL interaction on haze pollution: multiyear observational evidences in north China. Geophys. Res. Lett. 45, 8596–8603.
Hegg, D.A., Warren, S.G., Grenfell, T.C., Doherty, S.J., Larson, T.V., Clarke, A.D., 2009. Source attribution of black carbon in arctic snow. Environ. Sci. Technol. 43, 4016–4021.
Hoek, G., Krishnan, R.M., Beelen, R., Peters, A., Ostro, B., Brunekreef, B., et al., 2013. Long-term air pollution exposure and cardio-respiratory mortality: a review. Environ. Health 12.
Jacobson, M.Z., 2002. Control of fossil-fuel particulate black carbon and organic matter, possibly the most effective method of slowing global warming. J. Geophys. Res.-Atmos. 107.
Janssen, N.A., Gerlofs-Nijland, M.E., Lanki, T., Salonen, R.O., Cassee, F., Hoek, G., Fischer, P., Brunekreef, B., Krzyzanowski, M., 2012. Health Effects of Black Carbon. World Health Organization Regional Office For Europe.
Keohane, R.O., Victor, D.G., 2016. Cooperation and discord in global climate policy. Nat. Clim. Change 6, 570–575.
Koch, D., Schulz, M., Kinne, S., McNaughton, C., Spackman, J.R., Balkanski, Y., et al., 2009. Evaluation of black carbon estimations in global aerosol models. Atmos. Chem. Phys. 9, 9001–9026.
Kopacz, M., Mauzerall, D.L., Wang, J., Leibensperger, E.M., Henze, D.K., Singh, K., 2011. Origin and radiative forcing of black carbon transported to the Himalayas and Tibetan Plateau. Atmos. Chem. Phys. 11, 2837–2852.
Kopp, R.E., Mauzerall, D.L., 2010. Assessing the climatic benefits of black carbon mitigation. Proc. Natl. Acad. Sci. U. S. A. 107, 11703–11708.
Krewski, D., Jerrett, M., Burnett, R.T., Ma, R., Hughes, E., Shi, Y., Turner, M.C., Pope III, C.A., Thurston, G., Calle, E.E., Thun, M.J., 2009. Extended Follow-Up and Spatial Analysis of the American Cancer Society Study Linking Particulate Air Pollution and Mortailty. Health Effects Institute, Boston, MA HEI Research Report.
Lamarque, J.F., Bond, T.C., Eyring, V., Granier, C., Heil, A., Klimont, Z., et al., 2010. Historical (1850-2000) gridded anthropogenic and biomass burning emissions of reactive gases and aerosols: methodology and application. Atmos. Chem. Phys. 10, 7017–7039.
Lamarque, J.F., Dentener, F., McConnell, J., Ro, C.U., Shaw, M., Vet, R., et al., 2013a. Multi-model mean nitrogen and sulfur deposition from the Atmospheric Chemistry and Climate Model Intercomparison Project (ACCMIP): evaluation of historical and projected future changes. Atmos. Chem. Phys. 13, 7997–8018.
Lamarque, J.F., Shindell, D.T., Josse, B., Young, P.J., Cionni, I., Eyring, V., et al., 2013b. The Atmospheric Chemistry and Climate Model Intercomparison Project (ACCMIP): overview and description of models, simulations and climate diagnostics. Geosci. Model Dev. (GMD) 6, 179–206.
Lee, Y.H., Lamarque, J.F., Flanner, M.G., Jiao, C., Shindell, D.T., Berntsen, T., et al., 2013. Evaluation of preindustrial to present-day black carbon and its albedo forcing from atmospheric chemistry and climate model intercomparison project (ACCMIP). Atmos. Chem. Phys. 13, 2607–2634.
Li, C.L., Bosch, C., Kang, S.C., Andersson, A., Chen, P.F., Zhang, Q.G., et al., 2016. Sources of black carbon to the Himalayan-Tibetan Plateau glaciers. Nat. Commun. 7.
Li, F., Ginoux, P., Ramaswamy, V., 2008. Distribution, transport, and deposition of mineral dust in the Southern Ocean and Antarctica: contribution of major sources. J. Geophys. Res.-Atmos. 113.
Liu, J.F., Fan, S.M., Horowitz, L.W., Levy, H., 2011. Evaluation of factors controlling long-range transport of black carbon to the Arctic. J. Geophys. Res.-Atmos. 116.
Liu, J.F., Mauzerall, D.L., Horowitz, L.W., 2005. Analysis of seasonal and interannual variability in transpacific transport. J. Geophys. Res.-Atmos. 110.
Liu, J.F., Mauzerall, D.L., Horowitz, L.W., 2009a. Evaluating inter-continental transport of fine aerosols:(2) Global health impact. Atmos. Environ. 43, 4339–4347.
Liu, J.F., Mauzerall, D.L., Horowitz, L.W., Ginoux, P., Fiore, A.M., 2009b. Evaluating inter-continental transport of fine aerosols: (1) Methodology, global aerosol

distribution and optical depth. Atmos. Environ. 43, 4327–4338.
Mao, Y.H., Liao, H., Han, Y.M., Cao, J.J., 2016. Impacts of meteorological parameters and emissions on decadal and interannual variations of black carbon in China for 1980-2010. J. Geophys. Res.-Atmos. 121, 1822–1843.
McConnell, J.R., Edwards, R., Kok, G.L., Flanner, M.G., Zender, C.S., Saltzman, E.S., et al., 2007. 20th-century industrial black carbon emissions altered arctic climate forcing. Science 317, 1381–1384.
Morton, L., Chen, L., Gordon, T., Ito, K., Thurston, G.D., 2013. HEALTH EFFECTS INSTITUTE (HEI). National Particle Component Toxicity (NPACT) Initiative: Integrated Epidemiologic and Toxicologic Studies of the Health Effects of Particulate Matter Components.
Naik, V., Voulgarakis, A., Fiore, A.M., Horowitz, L.W., Lamarque, J.F., Lin, M., et al., 2013. Preindustrial to present-day changes in tropospheric hydroxyl radical and methane lifetime from the Atmospheric Chemistry and Climate Model Intercomparison Project (ACCMIP). Atmos. Chem. Phys. 13, 5277–5298.
Parrish, D.D., Lamarque, J.F., Naik, V., Horowitz, L., Shindell, D.T., Staehelin, J., et al., 2014. Long-term changes in lower tropospheric baseline ozone concentrations: comparing chemistry-climate models and observations at northern midlatitudes. J. Geophys. Res.-Atmos. 119, 5719–5736.
Paulot, F., Ginoux, P., Cooke, W.F., Donner, L.J., Fan, S., Lin, M.Y., et al., 2016. Sensitivity of nitrate aerosols to ammonia emissions and to nitrate chemistry: implications for present and future nitrate optical depth. Atmos. Chem. Phys. 16, 1459–1477.
Peng, J.F., Hu, M., Guo, S., Du, Z.F., Zheng, J., Shang, D.J., et al., 2016. Markedly enhanced absorption and direct radiative forcing of black carbon under polluted urban environments. Proc. Natl. Acad. Sci. U. S. A. 113, 4266–4271.
Qin, Y., Xie, S.D., 2011a. Estimation of county-level black carbon emissions and its spatial distribution in China in 2000. Atmos. Environ. 45, 6995–7004.
Qin, Y., Xie, S.D., 2011b. Historical estimation of carbonaceous aerosol emissions from biomass open burning in China for the period 1990-2005. Environ. Pollut. 159, 3316–3323.
Qin, Y., Xie, S.D., 2012. Spatial and temporal variation of anthropogenic black carbon emissions in China for the period 1980-2009. Atmos. Chem. Phys. 12, 4825–4841.
Ramanathan, V., Carmichael, G., 2008. Global and regional climate changes due to black carbon. Nat. Geosci. 1, 221–227.
Ramanathan, V., Chung, C., Kim, D., Bettge, T., Buja, L., Kiehl, J.T., et al., 2005. Atmospheric brown clouds: impacts on South Asian climate and hydrological cycle. Proc. Natl. Acad. Sci. U. S. A. 102, 5326–5333.
REVIHAAP, 2013. Review of Evidence on Health Aspects of Air Pollution – REVIHAAP Project. World Health Organization Technical Report.
Sand, M., Berntsen, T.K., von Salzen, K., Flanner, M.G., Langner, J., Victor, D.G., 2016. Response of Arctic temperature to changes in emissions of short-lived climate forcers. Nat. Clim. Change 6, 286.
Schnell, J.L., Prather, M.J., Josse, B., Naik, V., Horowitz, L.W., Cameron-Smith, P., et al., 2015. Use of North American and European air quality networks to evaluate global chemistry-climate modeling of surface ozone. Atmos. Chem. Phys. 15, 10581–10596.
Shen, Z.Y., Ming, Y., Horowitz, L.W., Ramaswamy, V., Lin, M.Y., 2017. On the seasonality of arctic black carbon. J. Clim. 30, 4429–4441.
Shindell, D., Kuylenstierna, J.C.I., Vignati, E., van Dingenen, R., Amann, M., Klimont, Z., et al., 2012. Simultaneously mitigating near-term climate change and improving human health and food security. Science 335, 183–189.
Shindell, D.T., Chin, M., Dentener, F., Doherty, R.M., Faluvegi, G., Fiore, A.M., et al., 2008. A multi-model assessment of pollution transport to the Arctic. Atmos. Chem. Phys. 8, 5353–5372.
Shindell, D.T., Lamarque, J.F., Schulz, M., Flanner, M., Jiao, C., Chin, M., et al., 2013. Radiative forcing in the ACCMIP historical and future climate simulations. Atmos. Chem. Phys. 13, 2939–2974.
Silva, R.A., West, J.J., Zhang, Y.Q., Anenberg, S.C., Lamarque, J.F., Shindell, D.T., et al., 2013. Global premature mortality due to anthropogenic outdoor air pollution and the contribution of past climate change. Environ. Res. Lett. 8.
Smith, K.R., Mehta, S., 2003. The burden of disease from indoor air pollution in developing countries: comparison of estimates. Int. J. Hyg Environ. Health 206, 279–289.
Stevenson, D.S., Young, P.J., Naik, V., Lamarque, J.F., Shindell, D.T., Voulgarakis, A., et al., 2013. Tropospheric ozone changes, radiative forcing and attribution to emissions in the atmospheric chemistry and climate model intercomparison project (ACCMIP). Atmos. Chem. Phys. 13, 3063–3085.
UNEP, 2011. Near-term Climate Protection and Clean Air Benefits: Actions for Controlling Short-Lived Climate Forcers. United Nations Environment Programme (UNEP).
UNEP/WMO, 2011. Integrated Assessment of Black Carbon and Tropospheric Ozone. United Nations Environment Programme (UNEP).
Voulgarakis, A., Naik, V., Lamarque, J.F., Shindell, D.T., Young, P.J., Prather, M.J., et al., 2013. Analysis of present day and future OH and methane lifetime in the ACCMIP simulations. Atmos. Chem. Phys. 13, 2563–2587.
Wang, H.L., Rasch, P.J., Easter, R.C., Singh, B., Zhang, R.D., Ma, P.L., et al., 2014. Using an explicit emission tagging method in global modeling of source-receptor relationships for black carbon in the Arctic: variations, sources, and transport pathways. J. Geophys. Res.-Atmos. 119, 12888–12909.
Winiger, P., Andersson, A., Eckhardt, S., Stohl, A., Gustafsson, O., 2016. The sources of atmospheric black carbon at a European gateway to the Arctic. Nat. Commun. 7.
Wang, Z.L., Huang, X., Ding, A.J., 2018. Dome effect of black carbon and its key influencing factors: a one-dimensional modelling study. Atmos. Chem. Phys. 18, 2821–2834.
Young, P.J., Archibald, A.T., Bowman, K.W., Lamarque, J.F., Naik, V., Stevenson, D.S., et al., 2013. Pre-industrial to end 21st century projections of tropospheric ozone from the atmospheric chemistry and climate model intercomparison project (ACCMIP). Atmos. Chem. Phys. 13, 2063–2090.
Zhang, J., Liu, J., Tao, S., Ban-Weiss, G.A., 2015a. Long-range transport of black carbon to the Pacific Ocean and its dependence on aging timescale. Atmos. Chem. Phys. 15, 11521–11535.
Zhang, R., Wang, H., Qian, Y., Rasch, P.J., Easter, R.C., Ma, P.L., et al., 2015b. Quantifying sources, transport, deposition, and radiative forcing of black carbon over the Himalayas and Tibetan Plateau. Atmos. Chem. Phys. 15, 6205–6223.
Zhao, M., Golaz, J.C., Held, I.M., Guo, H., Balaji, V., Benson, R., et al., 2018. The GFDL global atmosphere and land model AM4.0/LM4.0:2. Model description, sensitivity studies, and tuning strategies. J. Adv. Model. Earth Syst. 10, 735–769.
Zhao, Y., Nielsen, C.P., Lei, Y., McElroy, M.B., Hao, J., 2011. Quantifying the uncertainties of a bottom-up emission inventory of anthropogenic atmospheric pollutants in China. Atmos. Chem. Phys. 11, 2295–2308.
Zhang, Y., Ding, A.J., Mao, H.T., Nie, W., Zhou, D.R., Liu, L.X., Huang, X., Fu, C.B., 2016. Impact of synoptic weather patterns and inter-decadal climate variability on air quality in the North China Plain during 1980-2013. Atmos. Environ. 124, 119–128.

Further Reading

Fang, Y.Y., Fiore, A.M., Horowitz, L.W., Gnanadesikan, A., Held, I., Chen, G., et al., 2011. The impacts of changing transport and precipitation on pollutant distributions in a future climate. J. Geophys. Res.-Atmos. 116.